Journal of Materials Chemistry B

RSC Publishing

PAPER

View Article Online
View Journal | View Issue

A novel amperometric biosensor for hydrogen peroxide and glucose based on cuprous sulfide nanoplates

Cite this: *J. Mater. Chem. B*, 2013, **1**, 4127

Swarup Kumar Maji,†[a] Amit Kumar Dutta,[a] Gopala Ram Bhadu,[b] Parimal Paul,*[b] Anup Mondal*[a] and Bibhutosh Adhikary*[a]

Received 13th June 2013
Accepted 25th June 2013

DOI: 10.1039/c3tb20846j

www.rsc.org/MaterialsB

A facile, greener and template free route has been developed to produce cuprous sulfide (Cu_2S) nanoplates (NPs) with average diameters of 70–150 nm, *via* one step solvothermal decomposition of a single-source precursor (SSP) $Cu(ACDC)_2$ [ACDC = 2-aminocyclopentene-1-dithiocarboxylate] in the presence of ethylenediamine (EN) and triethylenetetramine (TETA) as structure orienting agents. The precursor complex and nanomaterials were thoroughly characterized by several common techniques and measurements, which give the composition and characteristics of the materials. Amperometric biosensors for hydrogen peroxide (H_2O_2) and glucose have been constructed by immobilizing the synthesized Cu_2S NPs in glutaraldehyde on a glassy carbon (GC) electrode using a direct drop-coating method. The proposed sensor has displayed faster response, high and reproducible sensitivity (64.27 μA mM^{-1}) with linear range of 10 μM to 3.75 mM, towards the electrochemical biosensing of H_2O_2 at −0.35 V (*vs.* Ag/AgCl). The sensor also showed high and reproducible sensitivity (61.67 μA mM^{-1}) towards glucose determination with linear range of 10 μM to 3.1 mM. The anti-inference ability of electroactive molecules and favorable stability are some of the advantages of the proposed sensor. Finally, using the sensor we have determined the glucose concentration in a human blood serum sample. The results strongly demonstrate the usefulness of Cu_2S NPs for biosensor design and other biological applications.

1 Introduction

Nanostructured materials have triggered tremendous motivation among scientists to explore the possibilities of using them in industrial and medical applications due to their unique and fascinating properties.[1] Biosensors are an essential tool in the fields of health care, chemical and biological analysis, environmental monitoring and good processing industries.[2] Among them, due to important clinical and industrial applications, glucose sensors, as one of the most popular biosensors, have been comprehensively investigated.[3] The fast and accurate determination of glucose has profound applications, since glucose concentration is a crucial indicator in many diseases, such as endocrine metabolic disorder and diabetes. Diabetes mellitus is a group of metabolic disease affecting millions of people over the world. This metabolic disorder results from insulin deficiency and hyper- and hypo-glycemia is reflected by blood glucose concentrations higher or lower than the normal range 4.4–6.6 mM.[3] The disease is one of the leading causes of death and disability in the world. These deaths and disabilities can be reduced through effective personal control of glucose in blood. Accordingly, diagnosis and management of diabetes through strict monitoring of blood glucose level is of paramount importance and millions of diabetics test their blood glucose levels daily, making glucose the most commonly tested analyte. Henceforth, the rising demand for glucose sensor with high sensitivity, high reliability, fast response and excellent selectivity has driven incredible research interest for decades.[4,5] Many efforts have been made to develop reliable glucose biosensor, such as electrochemical methods,[6] chemiluminescence,[7] or other methods.[8] Among all of the methods, amperometric glucose biosensor has drawn the most interest because of its simplicity, high selectivity and cost effectiveness.[9–11] Accordingly, it has played a leading role in the move toward simple, easy-to-use blood sugar testing and is expected to play a similar role in the move toward continuous glucose monitoring. Although significant research effort has been made to fabricate glucose biosensors, the development of a reliable cost effective glucose biosensor should play a leading role in the field of medical diagnostics and biotechnology.

A considerable interest to the operation of oxides-based amperometric biosensors has also been made, since H_2O_2 will be produced during the enzyme/glucose reaction. The glucose

[a]*Department of Chemistry, Bengal Engineering and Science University, Shibpur, Howrah 711 103, West Bengal, India. E-mail: anupmondal2000@yahoo.co.in; bibhutoshadhikary@yahoo.in; Fax: +91-3326682916; Tel: +91-3326684561*

[b]*Department of Analytical Sciences, Central Salt & Marine Chemicals Research Institute, Gijubhai, Badheka Marg, Bhavnagar 364002, Gujarat, India*

† Present address: Department of Physical and Mathematical Sciences, Nanyang Technological University, 21 Nanyang Link, 637371, Singapore.

oxidase (GOD) in reaction medium can chemically catalyze the oxidation of glucose to gluconolactone and H_2O_2, by the assistance of oxygen. Since the amount of glucose is proportional to that of the produced H_2O_2, as a result, the concentration of glucose can be indirectly detected by determining the liberated H_2O_2 in the reaction.[12]

$$\text{Glucose} + O_2 \xrightarrow{\text{GOD}} \text{Gluconolactone} + H_2O_2$$

$$H_2O_2 \rightarrow 2H^+ + O_2 + 2e^- \text{ (oxidation)}$$

$$H_2O_2 + 2H^+ + 2e^- \rightarrow 2H_2O \text{ (reduction).}$$

By following the above mentioned reaction mechanism, a wide range of amperometric enzyme electrodes based on nanomaterials have been discovered for use as glucose sensors by differing in electrode design or material, immobilization approach or membrane composition.[12–16] In connection to this, several nanostructured materials have been deposited on the electrode surface for the direct and indirect determination of H_2O_2.[17–29] Very recently, Cu_2S/OMCs nanocomposite modified GC electrode has been used for amperometric sensor of H_2O_2,[30] whereas, CuS–Nafion/GC electrodes as amperometric sensor of glucose.[31,32] However, to the best of our knowledge, Cu_2S nanoplates modified GC electrodes has not been used as sensors for H_2O_2 and glucose.

Among the Cu_xS compounds family including chalcocite (Cu_2S), djurleite ($Cu_{1.9375}S$), anilite ($Cu_{1.75}S$) and covellite (CuS), *etc.*, Cu_2S is of great interest due to its special properties and potential applications. Cu_2S is a p-type semiconductor, with a direct band gap of 1.2 eV.[33] It can be used in solar cells,[34] thin films of solar control coating with selective reflection of radiation,[35] thin-film transistor for panel displays,[36] electronic and optoelectronic chips,[37] biosensors,[38] cold cathodes[39] *etc.* There have been some excellent reports on the synthesis of Cu_2S nanocrystals with diverse shapes such as grains, flakes, rods and flower-like dendrites.[40–43] Because it has several advantages,[43] we have chosen the solvothermal decomposition of single-source precursor route over all other methods.

Herein, the ACDC complex of Cu(II) [$Cu(ACDC)_2$] has been utilized as an effective SSP for the preparation of Cu_2S NPs using a solvothermal technique. Cu_2S NP-modified GC electrodes were then constructed to study their potential applications as amperometric biosensors towards H_2O_2 and glucose and promising results have been found. Finally, the interference ability (selectivity) and applicability towards the measurement of glucose concentration in a diluted serum sample of human blood have been investigated.

2 Experimental

Chemicals and materials

The chemicals used for the preparation of ammonium 2-aminocyclopentene-1-dithiocarboxylate [$NH_4(ACDC)$] were of analytical grade and used as received. $CuCl_2 \cdot 2H_2O$, ethylenediamine (EN), triethylenetetramine (TETA), hydrogen peroxide (H_2O_2), D-(+)-glucose, glucose oxidase (GOD), uric acid (UA), ascorbic acid (AA), L-cysteine (Cys), acetaminophen (AAP), glutathione (GSH) and *ortho*-phosphoric acid used as received. Millipore water, methanol, ethanol and diethyl ether were used as solvents.

Synthesis of precursor

The precursor complex was synthesized using ammonium 2-aminocyclopentene-1-dithiocarboxylate, $NH_4(ACDC)$ as the chelating ligand, by the previously reported method.[44] In a typical synthesis of $Cu(ACDC)_2$ complex, 86 mg of $CuCl_2 \cdot 2H_2O$ (0.5 mmol) was added to a 10 mL aqueous solution of $NH_4(ACDC)$ (176 mg, 1 mmol). A brown precipitate was obtained immediately. The product was isolated by filtration and washed with warm water followed by absolute ethanol and diethyl ether and then dried in air.

Anal. ($C_6H_{12}N_2S_2Cu$) calc.: C, 37.92; H, 4.27; N, 7.48. Found: C, 38.60; H, 4.34; N, 7.33. FT-IR (KBr, cm^{-1}): 3446 br, 3360 s (νN–H), 3251 m, 3176 m, 2925 m, 1612 s (δNH_2), 1506 m, 1454 ($\delta CH_2 + \nu C{=}C$), 1413 w, 1309 m ($\nu C{-}N + \nu C{=}S$), 1282 m ($\nu C{=}S + \nu CN$), 1119 m, 912 w (ν_{assym} CSS), 792 w, 620 w (ν_{sym} CSS), 512 w, 460 w, 416 w.

Preparation of Cu_2S NPs

Cu_2S NPs were prepared by solvothermal decomposition of the synthesized precursor complex [$Cu(ACDC)_2$] using two nucleophilic solvents, *viz.* EN and TETA in the following way.

(i) 1.0 g of precursor was dissolved in 20 mL EN in a round bottom flask. The resultant deep brown solution was heated at 110 °C for 20 min. The suspension was then cooled to room temperature and about 20 mL of methanol was added to it. The as deposited black precipitate was centrifuged and washed several times with methanol for purification and then annealed at 250 °C under N_2 atmosphere for 30 min.

(ii) In the case of TETA, 1.0 g of precursor was dissolved in 20 mL TETA in a round bottom flask. The resultant deep brown was heated at 150 °C for 20 min. The resultant black suspension was then cooled to room temperature and about 20 mL of methanol was added to it. The as deposited black precipitate was centrifuged and washed several times with methanol for purification and then annealed at 250 °C under N_2 atmosphere for 30 min.

Physical measurements

Elemental analyses (C, H and N) were carried out by a Perkin-Elmer 2400II instrument. FTIR spectrum was recorded on a JASCO FTIR-460 Plus spectrophotometer. UV-Visible absorption spectra were observed on a JASCO V-530 UV-VIS spectrophotometer. Powder X-ray diffraction (XRD) patterns were obtained on a Philips PW 1140 parallel beam X-ray diffractometer with Bragg–Bretano focusing geometry and monochromatic CuKα radiation (λ = 1.540598 Å). Transmission electron microscopy (TEM) images and selected area diffraction (SAED) patterns were collected by using JEOL JEM-2100 microscope working at 200 kV. Electrochemical measurements were monitored using CHI 620D electrochemical analyzer.

Electro-catalytic activity towards hydrogen peroxide and glucose

At first Cu_2S NPs/GC electrodes were fabricated for several electrochemical measurements. A GC electrode (3 mm in diameter) was polished to a mirror-like finish with fine emery papers and 1.0 and 0.05 μM alumina slurry followed by rinsing thoroughly with Milli-Q water. 5 mg Cu_2S NPs was dispersed in 50 μL glutaraldehyde and then ultrasonicated for 1 h 20 μL of colloidal suspension was dropped on the GC electrode surface and dried at room temperature for over night.

Electrochemical measurements were carried out in a cell containing 20 mL of 0.1 M PBS (pH 7.4, 30 °C) at a scan rate of 0.1 V s^{-1}. In a typical cell setup, platinum wire was used as an auxiliary electrode, an Ag/AgCl electrode as reference and Cu_2S NPs modified GC (Cu_2S NPs/GC) as the working electrodes. Electrochemical impedance spectroscopy (EIS) was carried out in a beaker containing 40 mL 0.1 M KCl with 5 mM $Fe(CN)_6^{4-/3-}$ (1 : 1) solution in the frequency range 0.1 Hz to 10.0 kHz using similar electrode setup.

For electrochemical measurements towards glucose detection, the same electrode setup was used with an applied potential of −0.35 V (*vs.* Ag/AgCl) at a scan rate of 0.1 V s^{-1}, however, the electrolyte solution was 0.1 M PBS containing 1 mg mL^{-1} GOD (pH 7.4, 30 °C).

3 Results and discussion

The brown precursor complex was synthesized by the reaction of $CuCl_2 \cdot 2H_2O$ with NH_4(ACDC) (1 : 2) in aqueous medium at room temperature. The precursor complex is air stable and insoluble in water and common organic solvents, however, readily soluble in DMF and DMSO. The synthesized precursor complex was characterized by C, H and N elemental analyses and FTIR spectroscopic measurements. The measured CHN elemental analysis of SSP with proposed molecular formula [Cu(ACDC)$_2$] was in good agreement with the calculated values (calc.: C, 37.92; H, 4.27; N, 7.48. Found: C, 38.60; H, 4.34; N, 7.33%). The FTIR spectrum of Cu(ACDC)$_2$ complex was compared with the reported FTIR spectral bands which also supported the formation of precursor complex.[44] The Cu_2S nanoplates of were prepared by one step solvothermal decomposition of the precursor complex using two different nucleophilic solvents, such as EN and TETA in the temperature range 110–150 °C.

Structural characterization of Cu_2S NPs

The powder X-ray diffraction patterns of Cu_2S NPs obtained using EN and TETA are shown in Fig. 1. The 2θ values of the peaks observed were 28.04 for (2 6 2), 29.30 for (1 2 4), 32.44 for (4 3 1), 46.55 for (6 1 1), 47.65 for (1 14 1), 55.39 for (6 8 2), 68.89 for (6 8 6) and 73.20 for (0 20 3). All the reflection peaks were carefully compared to the Joint Committee on Powder Diffraction Standards (JCPDS) database and identified as the formation of the chalcocite (monoclinic) phase of Cu_2S (JCPDS no. 230961). The intensity of the peaks was considerably strong, which indicates that the products are well-crystallized. No

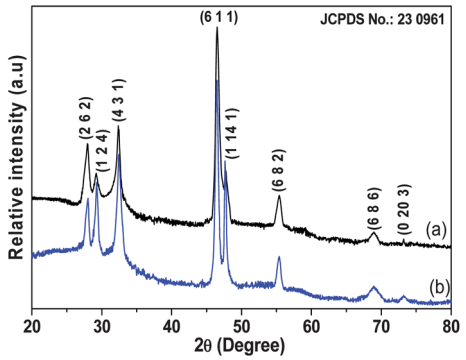

Fig. 1 Powder XRD of Cu_2S NPs prepared using (a) EN and (b) TETA.

characteristic peaks arising from the possible impurities were visible, such as CuO, Cu_2O and other phases of Cu_xS. This clearly indicates that pure crystalline chalcocite phase of Cu_2S was formed *via* a solvothermal decomposition of SSP. The diffraction peaks were broad, which indicates the formation of nano-sized particles. Crystal diameters for Cu_2S NPs were calculated using the Debye–Scherrer equation [$D = 0.9\lambda/(\beta\cos\theta)$, where, D is the crystallite size, λ is the wave length of X-ray (1.540598 Å), β is the value of full width at half maximum and θ is the Bragg's angle] and found to be 5.3 and 7.6 nm prepared using EN and TETA, respectively.

The structural characterization of Cu_2S NPs was also carried out using transmission electron microscopy (TEM), selected area electron diffraction (SAED), Live Fast-Fourier Transform (FFT) and the images are shown in Fig. 2. As shown in Fig. 2a(i) and b(i), the images showed the formation of irregular shape nanoplates with clear edges of average diameter 70 nm in case of EN and 150 nm in case of TETA, as reacting solvents. The average particle sizes as obtained from TEM images are higher than those of the XRD results, which was due to aggregation of the newly generated crystal nuclei.

Plate like Cu_2S has been obtained in both cases; however, the size of the product strongly depends on the reacting solvent. The anisotropic growth of the Cu_2S nanoplates may be originated from the crystalline facets which tend to develop on the low-index planes to minimize the surface energy when growing.[45] Moreover, it can be concluded that EN and TETA play the key role for the formation of these anisotropic plates and similar observations have been reported previously.[46] Since it is well established that these type of chemicals not only act as solvents but also act as an attacking nucleophile for the breakdown of precursor complex as well as a capping agent for the preparation of different kinds of nanoparticles.[26,28]

The SAED patterns of Cu_2S NPs prepared using EN and TETA are displayed in Fig. 2a(ii) and b(ii), respectively. The diffraction patterns were exactly matched with the chalcocite phase of Cu_2S (JCPDS no. 230961). A set of well defined concentric rings were evident from the SAED patterns, which suggest the formation of crystalline materials of lower dimension. On the other hand, high resolution TEM (HRTEM) images of nanoplates, which were under consideration (Fig. 2a(iii) and b(iii)) displayed high-quality lattice fringes of nanocrystals, also indicating the good

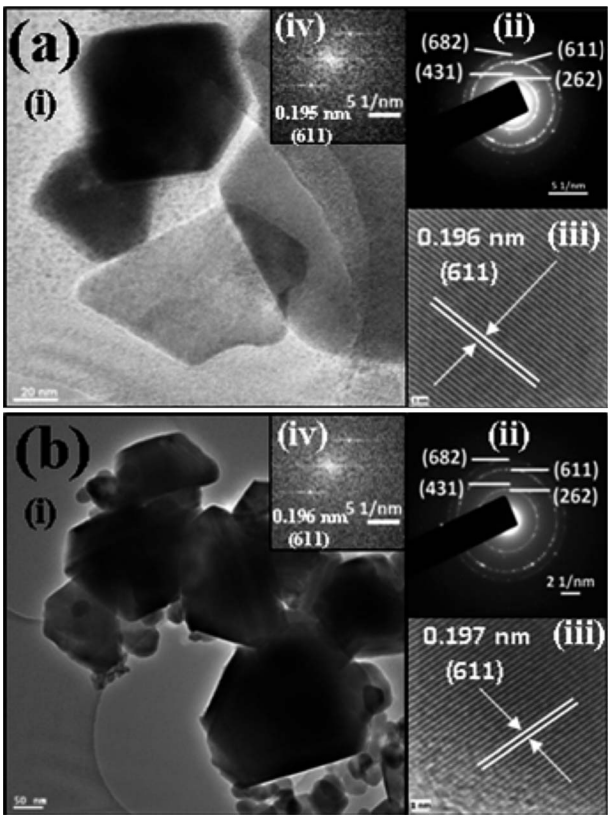

Fig. 2 (i) TEM, (ii) SAED, (iii) HRTEM and (iv) live FFT images of Cu_2S NPs prepared using (a) EN and (b) TETA.

crystalline nature of the products. Furthermore, the HRTEM images revealed that the NPs were grown preferentially along the (611) direction. The growth orientation was also supported by the Live FFT images as shown in Fig. 2a(iv) and b(iv).

Optical properties

Optical property of Cu_2S NPs was investigated by the UV-vis absorption spectroscopic measurements and the corresponding plots are shown in Fig. 3. The room temperature absorption spectra were recorded by dispersing the samples in water. The spectra showed sharp onset in absorbances at around 700 and 713 nm for Cu_2S NPs obtained using EN and TETA, respectively, due to the band-to-band transition of Cu_2S. Band gap energies (E_g) of Cu_2S NPs were calculated from the band edge absorption using the Tauc's relation. As Cu_2S is an indirect band gap semiconductor,[33] therefore, the value of E_g can be evaluated, from the plot of $(\alpha h\nu)^{1/2}$ *vs.* $h\nu$ and shown in the inset of Fig. 3. From the Tauc's plot the band gap energy of Cu_2S NPs were turn out be 1.97 (from EN) and 1.87 (from TETA) eV, which are blue shifted relative to the characteristic band gap energy of the bulk Cu_2S ($E_g = 1.2$ eV)[33] and may be due to the quantum confinement effect. Moreover, the band gap energy of the Cu_2S NP obtained from EN showed higher amount of blue shift due to smaller in size as observed from XRD and TEM measurements.

Electrochemical sensing of H_2O_2

The electro-catalytic activity towards the electrochemical reduction of H_2O_2 was studied with the modified Cu_2S NPs on GC electrode surface (Cu_2S NPs/GC) by cyclic voltammogram (CV) and chronoamperometric (CA) techniques. The typical CV curves of bare GC, Cu_2SNP(EN)/GC and Cu_2SNP(TETA)/GC electrodes in 0.1 M PBS (pH 7.4, 30 °C at scan rate of 0.1 V s^{-1}) are shown in Fig. 4a. It has been shown that the bare GC electrode did not show any significant current response (Fig. 4a(i)), while a drastic enhancement in electrochemical response of Cu_2SNP/GC electrodes were observed with a strong reduction peak at −0.35 V (*vs.* Ag/AgCl) (Fig. 4a(ii) and (iii)), indicating an obvious electro-catalytic response of the modified electrodes in aqueous medium and that they can be useful as a biosensor. The excellent electrochemical behavior of Cu_2S NPs may be due to the smaller size, larger surface area and superior electron transfer capability.

As shown in Fig. 4a, between the two types of Cu_2S NPs, the one that was prepared using EN showed two times higher current response than that prepared from TETA. The difference between the electro-catalytic activity of Cu_2SNP(EN)/GC and Cu_2SNP(TETA)/GC electrodes is due to the enhanced electron transfer capability of Cu_2SNP(EN)/GC electrode as measured in electrochemical impedance spectroscopy (EIS) (Fig. 4b), which may be due to the presence of smaller nanoplates and a higher specific surface area (17.53 m^2 g^{-1} for Cu_2SNPs prepared by EN and 10.38 m^2 g^{-1} prepared by TETA). It was shown that the Cu_2SNP(EN)/GC (84.7 Ω) electrode has a lower charge-transfer

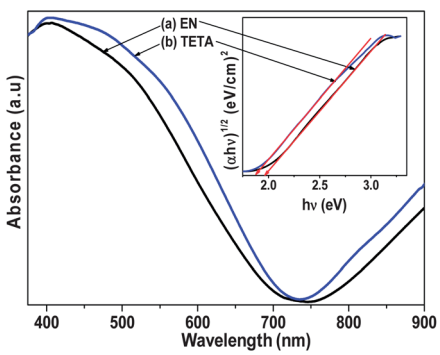

Fig. 3 UV-vis absorption spectra and the inset shows the corresponding $(\alpha h\nu)^{1/2}$ *vs.* $h\nu$ plot of Cu_2S NPs prepared using (a) EN and (b) TETA.

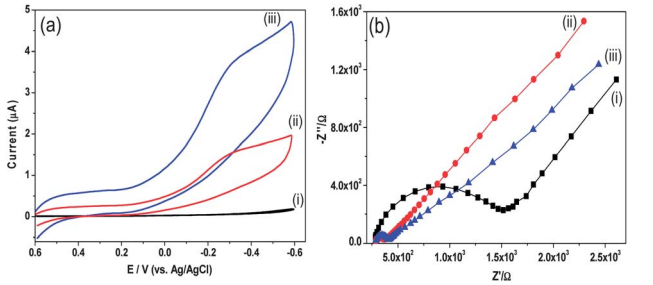

Fig. 4 (a) CV curves in PBS and (b) Nyquist plots in 0.1 M KCl containing 5 mM $Fe(CN)_6^{4-/3-}$ (1 : 1) solution of (i) GC, (ii) Cu_2SNP(EN)/GC and (iii) Cu_2SNP(TETA)/GC electrodes.

resistance value than that of Cu_2SNP(TETA)/GC (133.4 Ω), demonstrating that Cu_2SNP(EN)/GC has higher electrochemical activity than Cu_2SNP(TETA)/GC. Therefore, the further investigations on sensing properties have been carried out using Cu_2SNP(EN)/GC as the working electrode. In addition, the effect of solution pH (5.0 to 9.0) and temperature (25–100 °C) on the electrocatalytic activity of the modified electrode were studied in PBS under similar conditions. It can be seen from Fig. 5 that the reduction peak current changed gradually with an increasing pH and reached the maximum response at pH 7.4. On the other hand, in case of temperature profile, it was revealed that the electrode response gradually increased with increasing temperature and reached its maximum value at 90 °C. In order to obtain maximum sensitivity, pH 7.4 was chosen in subsequent experiments, which is the biological pH and also for human blood, whereas, all the experiments were carried out at room temperature (30 °C). Therefore, the robustness of Cu_2S NPs makes them suitable for a broad range of applications in the fields of biomedicine and environmental chemistry.

The electrochemical sensing behavior of the Cu_2SNP(EN)/GC electrode towards H_2O_2 was further studied by CV measurements with the successive addition of H_2O_2 (20, 40 and 60 μM) to 0.1 M PBS (pH 7.4, 30 °C) at scan rate of 0.1 V s^{-1}. As shown in Fig. 6, the cathodic peak current at −0.35 V increased significantly and linearly on addition of H_2O_2, which indicates an obvious electrocatalytic reduction of H_2O_2. Furthermore, the typical diffusion-controlled electrochemical behavior was also established by the CV profiles of Cu_2SNP(EN)/GC electrode in PBS with 20 μM H_2O_2 obtained at different scan rates. It has been observed that the reduction peak current increased linearly with square root of the scan rate in the range of 20–800 mV s^{-1} (Fig. 7). It is also interesting to note that the potential of reduction peak was shifted to the negative direction with increasing scan rate, which is mainly associated with the internal resistance of the electrode. Henceforth, the results suggest superior sensing application of Cu_2S NPs in aqueous solution towards H_2O_2.

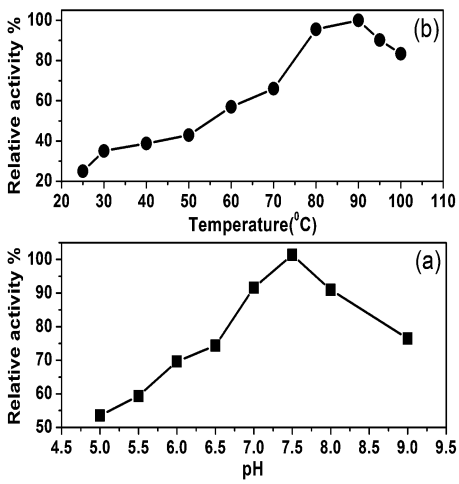

Fig. 5 The effect of (a) pH and (b) temperature on the electrocatalytic activity of Cu_2SNP(EN)/GC electrode in PBS (*vs.* Ag/AgCl).

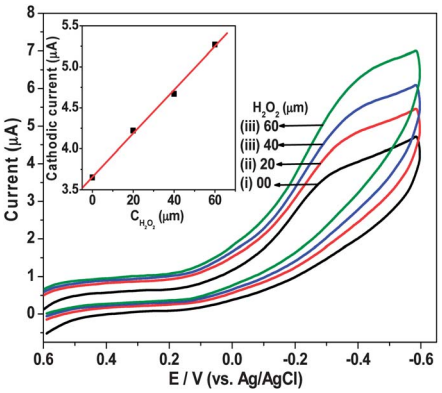

Fig. 6 CV curves for the Cu_2SNP(EN)/GC electrode upon successive addition of H_2O_2 to PBS (*vs.* Ag/AgCl) and the inset shows the calibration plot (scan rate of 0.1 V s^{-1}).

The quantitative estimation of H_2O_2 in an aqueous medium was further carried out using the CA technique with a Cu_2SNP(EN)/GC electrode under a similar cell setup and experimental conditions at −0.35 V. The current response of the modified electrode with successive addition of H_2O_2 to PBS is displayed in Fig. 8a, which showed a stepwise increment of the current with addition of H_2O_2. The electrode achieved 95% of the steady-state-current within 5 s. This result indicates vary fast electrocatalytic response of the Cu_2SNP(EN)/GC electrode. The calibration plot (Fig. 8b) of the current–time response curve showed that it has a linear relationship in the range of 10 μM to 3.75 mM, with a correlation coefficient of 0.99958, which is much wider than 1.76–139 μM for NCNT/GC,[12] 0.5–150 μM for sheet-like FeS/GC,[21] 0.5 μM to 1.3 mM for FeS/FTO,[27] 10 μM to 1.5 mM for MnO_2/Nafion/GC,[19] 1 μM to 1.9 mM for CdS/GC,[28] 1 μM to 3.03 mM for Cu_2S/OMCs/Nafion/GC,[30] electrodes and several recently reported sensors.[20,23] From the calibration curve, the sensitivity of the sensor was estimated to be 64.27 μA mM^{-1}, which is similar to or even better than that of the above mention fabricated electrodes. The lower limit of detection of the sensor was found to be 1.1 μM ($S/N = 3$), which is lower than MnO_2/Nafion/GC,[19] Co_3O_4/GC electrode,[20] however slightly

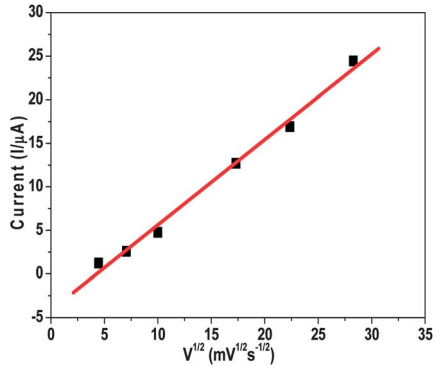

Fig. 7 The linear relationship between the reduction peak current (−0.35 V) and the square of scan rates (scan rates: 20, 50, 100, 300, 500, 600 mV s^{-1}) for Cu_2SNP(EN)/GC electrode in 0.1 M PBS with 20 μM H_2O_2.

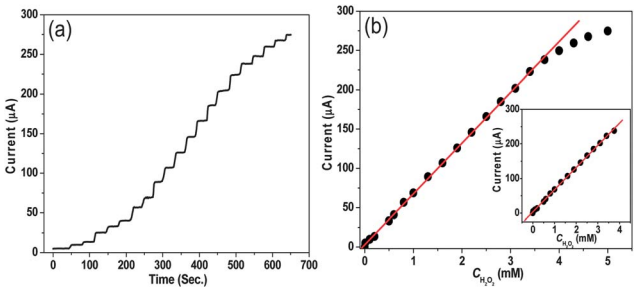

Fig. 8 (a) Amperometric response and (b) calibration plot and in the inset a Lineweaver–Burk plot for the Cu_2SNP(EN)/GC electrode with successive addition of H_2O_2 to PBS at −0.35 V (*vs.* Ag/AgCl).

higher than the above reported sensors. By comparing the analytical parameters with the reported literature, we have found that the Cu_2S NP-modified GC electrode demonstrates attractive performance as a H_2O_2 sensor and can be useful in biosensing devices.

Electrochemical sensing of glucose

The electro-catalytic activity of the Cu_2SNP(EN)/GC electrode was further investigated by the detection and quantification of glucose using CV and CA techniques. Actually, the detection of glucose was made indirectly by monitoring the reduction of H_2O_2 in an aqueous medium, since H_2O_2 was liberated by the reaction of glucose and oxygen in the presence of glucose oxidase.[12]

Fig. 9a displays the CV curves of a Cu_2SNP(EN)/GC electrode with and without addition of glucose to 0.1 M PBS (pH 7.4, 30 °C) containing 1 mg mL^{-1} GOD at a scan rate of 0.1 V s^{-1}. It can be seen that the cathodic peak current at −0.35 V was increased from 3.89 to 4.60 μA with the addition of 30 μM glucose, indicating that Cu_2S NPs exhibit strong electrocatalytic activity in response to glucose oxidation and improve the electron transfer between glucose and GC electrode. Furthermore, the reduction peak current increased extensively and linearly with successive addition of glucose (30, 60 and 90 μM) to PBS containing GOD, indicating that Cu_2S NPs based sensor is sensitive to the concentration of glucose.

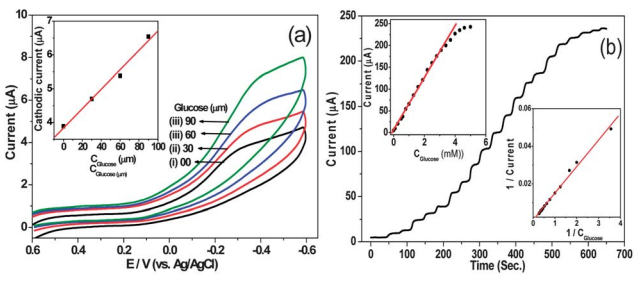

Fig. 9 (a) CV curves upon successive addition of glucose, the inset shows the calibration plot and (b) amperometric response, the insets show the calibration plot and Lineweaver–Burk plot for Cu_2SNP(EN)/GC electrode with successive addition of glucose to PBS containing 1 mg mL^{-1} GOD at −0.35 V (*vs.* Ag/AgCl).

To study several analytical parameters and the use as an amperometric biosensor towards glucose, CA measurement was further carried out using the Cu_2SNP(EN)/GC as a working electrode under a similar cell setup and experimental conditions at −0.35 V. As shown in Fig. 9b, the current–time response plot revealed that the biosensor exhibited a rapid and sensitive response to the change of glucose concentration from 10 μM to 5 mM, with an obvious increase in current response. The sensor achieved 95% of the steady-state-current within less than 10 s, suggesting a fast and good electron transfer electrocatalytic process. From the calibration plot, shown in the upper left inset of Fig. 9b, the electrode showed that it has a linear range of glucose concentration from 10 μM to 3.1 mM (correlation coefficient of 0.99916), with a lower limit of detection of about 1.3 μM. The sensitivity was also estimated as 61.67 μA mM^{-1}. These analytical parameters are attractive and comparably much higher than those of any CuS based,[31,32] NCNT/GC[12] and ZnO nanorods/Au hybrid nanocomposite[13] glucose biosensors, but lower than those of recently reported ZnO based sensors.[15,16] The enhanced electrocatalytic activity towards glucose sensing may be due to the higher specific surface area and better electron transfer of the proposed sensor based on Cu_2S nanoplates.

The calibration curve for Cu_2SNP(EN)/GC electrode showed that the electrocatalytic current (i_{cat}) increased linearly with successive addition of glucose and then reached a steady state position after a certain period (upper left inset of Fig. 9b). This calibration curve follows a typical Michaelis–Menten mechanism, from which the apparent Michaelis–Menten constant (K_m^{app}) can be obtained by using the Lineweaver–Burk model: $1/I_{ss} = 1/I_{max} + K_m^{app}/(I_{max} \times [S])$, where I_{ss} is the steady-state current, I_{max} the maximum current measured under conditions of enzyme saturation, [S] is the concentration of substrate (lower right inset of Fig. 9b). This Michaelis–Menten constant is used to evaluate the biological activity the biosensor. The K_m^{app} value was estimated to be 1.8 mM, which is lower than that of recently reported glucose sensors based on ZnO nanotubes (19 mM),[15] ZnO:Cu nanoclusters (21 mM),[47] and nano-$CaCO_3$ (21.4 mM).[48] This K_m^{app} value suggests that the Cu_2S NP-based biosensor possesses an attractive performance for glucose detection. However, for any oxidoreductase enzyme kinetics, in order to get a good liner range, the goal should be to make the K_m^{app} for glucose as large as possible (∼40–50 mM).

In the real application of any developed sensor for glucose, the required liner range should be ∼4–20 mM. In this context, our developed sensor has a little bit lower liner range detection capability. However, we are able to verify the workability of the proposed sensor in a real sample. The as-prepared Cu_2S NP-based sensor was used for the determination of glucose concentration in human blood sample. According to our investigation, the measured concentration of glucose in human blood is 5.67 mM (101.7 mg dL^{-1}) as shown in Fig. 10 and consistent with the value obtained from a pathological laboratory [5.88 mM (106.0 mg dL^{-1})]. The results prove that our prepared Cu_2S nanoplates based electrode would have a potential application in glucose sensor and any other biosensor devices.

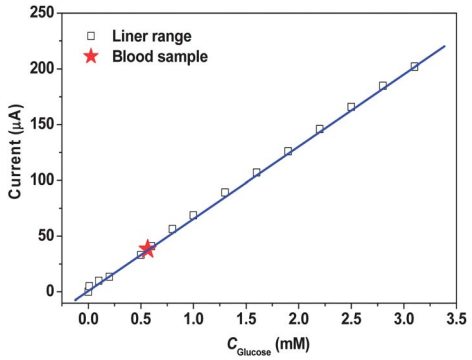

Fig. 10 The increase in current as a function of glucose concentration of Cu_2SNP(EN)/GC (black square and blue line) and the star is the current response after the addition of the blood sample to PBS.

Selectivity (anti-interference), reproducibility and stability

In measurements in real samples some electroactive species in the serum may influence the performance of the biosensor. Therefore, the selectivity and anti-interference ability of the biosensor was investigated by addition of specific amounts of electroactive species, such as UA (0.1 mM), AA (0.1 mM), L-Cys (0.05 mM), AAP (0.1 mM) and GSH (2 mM), during the current response measurement of 100 μM glucose in 0.1 M PBS containing 1 mg mL^{-1} GOD, shown in Fig. 11. No obvious current responses were observed with the addition of a certain amount of those electroactive interfering chemicals to PBS containing GOD. This result indicates that the proposed glucose sensor showed good anti-interference ability *i.e.* selectivity.

The reproducibility of the proposed sensor was also studied by adding a fixed amount of glucose (100 μM) to PBS containing GOD. The relative standard deviation (RSD) of the sensor response was 3.6% for five successive measurements for the same electrode. When the FeS/FTO electrode was stored at 4 °C for one month, the current response remained at 95% of its original value, suggesting the long-term stability of the electrode.

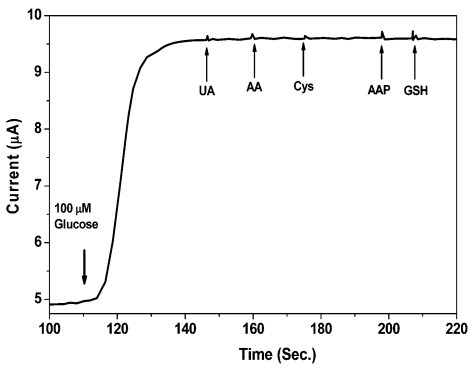

Fig. 11 CA response of the Cu_2SNP(EN)/GC electrode to successive addition of 100 μM glucose and uric acid (UA, 0.1 mM), ascorbic acid (AA, 0.1 mM), L-cysteine (Cys, 0.05 mM), acetaminophen (AAP, 0.1 mM), and glutathione (GSH, 2 mM) to PBS containing 1 mg mL^{-1} GOD.

4 Conclusions

A Cu(II) complex of 2-aminocyclopentene-1-dithiocarboxylate has been utilized for the preparation of Cu_2S nanoplates. Different sizes of nanoplates (70 and 150 nm) were obtained by one-step solvothermal decomposition of the precursor using EN and TETA as structure orienting solvents. These Cu_2S NPs anchored on GC surface have been applied for the electrochemical reduction and amperometric biosensor for H_2O_2 in aqueous solution and have shown favorable responses. A significant linear relationship could be obtained between the current density and the concentration of H_2O_2 from 10 μM to 3.75 mM, suggesting successful construction of a sensor for the detection of H_2O_2 in this concentration range, with a sensing time of 5 s. The sensitivity of the sensor was determined to be 64.27 μA mM^{-1} and the lower limit of detection was 1.1 μM. The fabricated biosensor was also applied for the electrochemical detection and amperometric sensing of glucose under similar conditions. Several electrochemical parameters *viz.* response time, linear range, sensitivity and lower limit of detection towards glucose concentration were calculated and showed similarity with those of H_2O_2. Finally, the selectivity, stability and ability to measure the real sample such as glucose concentration in human blood, suggest that our synthesized Cu_2S NPs are good nanostructured materials for potential application in biosensor devices and other biological applications.

Acknowledgements

A. K. Dutta is indebted to CSIR, India, for his RA [F. no. 08/003(96)/2013-EMR-I]. The authors also acknowledge Mrs. Shampa Adhikary for donating blood samples for the experiments. Thanks are due to MHRD-India and UGC-SAP (India) for providing instrumental facilities to the Department of Chemistry, Bengal Engineering and Science University, Shibpur.

Notes and references

1 D. B. Mitzi, L. L. Kosbar, C. E. Murray, M. Copel and A. Afzali, *Nature*, 2004, **428**, 299.
2 N. A. Rakow and K. S. Suslick, *Nature*, 2000, **406**, 710.
3 J. Wang, *Chem. Rev.*, 2008, **108**, 814.
4 G. S. Wilson and R. Gifford, *Biosens. Bioelectron.*, 2005, **20**, 2388.
5 J. D. Newman and A. P. F. Turner, *Biosens. Bioelectron.*, 2005, **20**, 2435.
6 J. S. Ye, Y. Wen, W. D. Zhang, L. M. Gan, G. Q. Xu and F. S. Sheu, *Electrochem. Commun.*, 2004, **6**, 66.
7 L. Zhu, Y. Li, F. Tian, B. Xu and G. Zhu, *Sens. Actuators, B*, 2002, **84**, 265.
8 K. E. Shafer-Peltier, C. L. Haynes, M. R. Glucksberg and R. P. Van Duyne, *J. Am. Chem. Soc.*, 2003, **125**, 588.
9 D. Lee, J. Lee, J. Kim, H. B. Na, B. Kim, C. H. Shin, J. H. Kwak, A. Dohnalkova, J. W. Grate, T. Hyeon and H. S. Kim, *Adv. Mater.*, 2005, **17**, 2828.

10 X. L. Luo, J. J. Xu, Y. Du and H. Y. Chen, *Anal. Biochem.*, 2004, **334**, 284.
11 W. Zhao, J. J. Xu, C. G. Shi and H. Y. Chen, *Langmuir*, 2005, **21**, 9630.
12 X. Xu, S. Jiang, Z. Hu and S. Liu, *ACS Nano*, 2010, **4**, 4292.
13 Y. Wei, Y. Li, X. Liu, Y. Xian, G. Shi and L. Jin, *Biosens. Bioelectron.*, 2010, **26**, 275.
14 C. Li, Y. Su, S. Zhang, X. Lv, H. Xia and Y. Wang, *Biosens. Bioelectron.*, 2010, **26**, 903.
15 T. Kong, Y. Chen, Y. Ye, K. Zhang, Z. Wang and X. Wang, *Sens. Actuators, B*, 2009, **138**, 344.
16 M. Ahamad, C. Pan, Z. Luo and J. Zhu, *J. Phys. Chem. C*, 2010, **114**, 9308.
17 M. R. Guascito, E. Filippo, C. Malitesta, D. Manno, A. Serra and A. Turco, *Biosens. Bioelectron.*, 2008, **24**, 1057.
18 C. Xiang, Y. Zou, L. X. Sun and F. Xu, *Sens. Actuators, B*, 2009, **136**, 158.
19 L. Zhang, Z. Fang, Y. Ni and G. Zhao, *Int. J. Electrochem. Sci.*, 2009, **4**, 407.
20 W. Jia, M. Guo, Z. Zheng, T. Yyu, E. G. Rodriguez, Y. Wang and Y. Lei, *J. Electroanal. Chem.*, 2009, **625**, 27.
21 Z. Dai, S. Liu, J. Bao and H. Ju, *Chem.–Eur. J.*, 2009, **15**, 4321.
22 L. Zhang, Y. Zhai, N. Gao, D. Wen and S. Dong, *Electrochem. Commun.*, 2008, **10**, 1524.
23 C. Xiang, Y. Zou, L. X. Sun and F. Xu, *Sens. Actuators, B*, 2009, **136**, 158.
24 C. Y. Lin, Y. H. Lai, A. Balamurugan, R. Vittal, C. W. Lin and K. C. Ho, *Talanta*, 2010, **82**, 340.
25 X. Wang, K. Jiao and G. Li, *Electrochim. Acta*, 2011, **56**, 2828.
26 S. K. Maji, A. K. Dutta, P. Biswas, D. N. Srivastava, P. Paul, A. Mondal and B. Adhikary, *Appl. Catal., A*, 2012, **419–420**, 170.
27 S. K. Maji, A. K. Dutta, P. Biswas, B. Karmakar, A. Mondal and B. Adhikary, *Sens. Actuators, B*, 2012, **166–167**, 726.
28 S. K. Maji, A. K. Dutta, D. N. Srivastava, P. Paul, A. Mondal and B. Adhikary, *J. Mol. Catal. A: Chem.*, 2012, **358**, 1.
29 A. K. Dutta, S. K. Maji, A. Mondal, B. Karmakar, P. Biswas and B. Adhikary, *Sens. Actuators, B*, 2012, **173**, 724.
30 X. Bo, J. Bai, L. Wang and L. Guo, *Talanta*, 2010, **81**, 339.
31 X. Zhang, G. Wang, A. Gu, Y. Wei and B. Fang, *Chem. Commun.*, 2008, 5945.
32 J. Liu and D. Xue, *J. Mater. Chem.*, 2011, **21**, 223.
33 S. Gorai, D. Ganguli and S. Chaudhuri, *Mater. Chem. Phys.*, 2004, **88**, 383.
34 M. Savelli and T. J. Bougnot, *Top. Appl. Phys.*, 1979, **31**, 213.
35 J. Cardoso, O. Gomez-Daza, L. Ixtlilco, M. T. S. Nair and P. K. Nair, *Semicond. Sci. Technol.*, 2001, **16**, 123.
36 S. Y. Kim, D. S. Kim, B. T. Agn and H. B. Im, *J. Mater. Sci.: Mater. Electron.*, 1993, **4**, 178.
37 N. Pop, C. Nascu, V. Ionescu, E. Indrea and I. Bratu, *Thin Solid Films*, 1997, **307**, 240.
38 H. Lee, S. W. Yoon, E. J. Kim and J. Park, *Nano Lett.*, 2007, **7**, 778.
39 J. Chen, S. Z. Deng, N. S. Xu, S. Wang, X. Wen, S. Yang, C. Yang, J. Wang and W. Ge, *Appl. Phys. Lett.*, 2002, **80**, 3620.
40 Y. Wu, C. Wadia, W. Ma, B. Sadtler and A. P. Alivisatos, *Nano Lett.*, 2008, **8**, 2551.
41 T. H. Larsen, M. B. Sigman, A. Ghezelbash, R. C. Doty and B. A. Korgel, *J. Am. Chem. Soc.*, 2003, **125**, 5638.
42 Z. Zhuang, Q. Peng, B. Zhang and Y. Li, *J. Am. Chem. Soc.*, 2008, **130**, 10482.
43 I. J. L. Plante, T. W. Zeid, P. Yang and T. Mokari, *J. Mater. Chem.*, 2010, **20**, 6612.
44 S.-N. Choi and J. R. Wasson, *Inorg. Chem.*, 1975, **14**, 1964.
45 J. Goebl, Q. Zhang, L. He and Y. Yin, *Angew. Chem., Int. Ed.*, 2012, **51**, 552.
46 J. S. Jang, C. J. Yu, S. H. Choi, S. M. Ji, E. S. Kim and J. S. Lee, *J. Catal.*, 2008, **254**, 144.
47 Z. W. Zhao, X. J. Chen, B. K. Tay, J. S. Chen, Z. J. Han and K. A. Khor, *Biosens. Bioelectron.*, 2007, **23**, 63901.
48 D. Shan, M. Zhu, H. Xue and S. Cosnier, *Biosens. Bioelectron.*, 2007, **22**, 1612.

